Asynchronous Timing and Doppler Recovery in DSP Based DPSK Modems for Fixed and Mobile Satellite Applications

B. Koblents, M. Belanger, D. Woods and P.J. McLane
Department of Electrical Engineering
Queen's University, Kingston, ON, K7L 3N6
Telephone: (613) 545–2937
Fax: (613) 545–6866

ABSTRACT

While conventional analog modems employ some kind of clock wave regenerator circuit for sychronous timing recovery, in sampled modem receivers timing is recovered asynchronously to the incoming data stream, with no adjustment being made to the input sampling rate. All timing corrections are accomplished by digital operations on the sampled data stream and timing recovery is asynchronous with the uncontrolled, input A/D system. A good timing error measurement algorithm is a zero crossing tracker proposed by Gardner. Digital, speech rate (2400 – 4800 bps) M-PSK modem receivers employing Gardner's zero crossing tracker were implemented and tested and found to achieve BER performance very close to theoretical values on the AWGN channel. Nyguist pulse shaped modem systems with excess bandwidth factors ranging from 100% to 60% were considered. We can show that for any symmetric M-PSK signal set Gardner's NDA algorithm is free of pattern jitter for any carrier phase offset for rectangular pulses and for Nyquist pulses having 100% excess bandwidth. Also, the Nyquist pulse shaped system is studied on the mobile satellite channel, where Doppler shifts and multipath fading degrade the $\pi/4-$DQPSK signal. Two simple modifications to Gardner's zero crossing tracker enable it to remain useful in the presence of multipath fading.*

I. INTRODUCTION

Within the last decade, low cost digital signal processing systems have become available. As these devices have become more powerful, it has become practical and desirable to implement fully digital modems with almost all the communications features implemented as realtime firmware. Timing recovery is a vital function of any modem, without which digital communication is impossible. We consider the timing recovery problem in a voice rate, fully digital modem which has been implemented as real time firmware on Second Generation Digital Signal Processors. The modem consists of a series of 4800 bps uncoded DQPSK modems employing Raised Cosine pulse shaping with excess bandwidth factors (α) ranging from 100% to 60%. Our modem employs asynchronous timing recovery, whereby the modem receiver recovers timing phase from the oversampled input signal, leaving it's input A/D converter free running. Such timing recovery techniques for digitally implemented modems are discussed in [1]. Zero crossing tracker timing error detectors of the type described by Gardner [1][2], are used to complete the timing recovery loops. The modem is experimentally tested on the AWGN channel, simulating the behaviour on a fixed satellite communications link. We show how to implement Gardner's algorithm for digital application and present the first experimental results on its performance. Additionally, the 4800 bps modem is modified to incorporate Doppler correction mechanisms and $\pi/4-$DQPSK modulation to enable it to operate on the mobile satellite channel with non-linear amplifiers. These modifications are also tested in the laboratory. The performance of the 4800 bps modem family on the mobile satellite fading channel is examined with the use of computer simulations. In particular, it is demonstrated that the zero crossing tracker timing error detectors can remain useful on the fading channel with simple modifications to their structure.

* This research was supported by the Telecommunications Research Institute of Ontario (TRIO) and the Natural Sciences and Engineering Research Council of Canada (NSERC).

II. ASYNCHRONOUS TIMING RECOVERY

In traditional analog modems, timing recovery is accomplished by regenerating a local clock wave to be synchronous with the data clock, and uses this local clock wave to adjust the frequency and phase of the input A/D converters to be synchronous with the incoming data [1]. One example of this synchronous timing recovery is shown in Figure 1. In a fully digital implementation, on the other hand, the input sampling takes place at the A/D converter at the very front end of the system as shown in Figure 2 and the sampling rate can be asynchronous to the incoming data stream. This Figure shows our complete receiver which will be discussed in the sequel. In most cases, the input sampling rate is an integer multiple of the nominal symbol rate, but the receiver sampler is free running and never explicitly locked to the transmitter baud clock [1,3]. Timing correction is accomplished by aligning the decimator strobes shown in Figure 3, with the pulse peaks out of the matched filters.

In our implementation, the receiver samples are kept track of by a sample counter, which is incremented once per sampling period, in a modulo N fashion, with N being the number of samples per symbol. To align the data strobes with the matched filter pulse peaks, it is necessary to retard them by a sampling interval. That is accomplished by resetting the receiver sample counter to negative one instead of zero at the end of the symbol where the timing decision is made, resulting in the next symbol epoch being one sampling interval longer than nominal. This aligns the receiver decimator strobe with the transmitter data strobe. We refer to this as adding a sample and it represents a negative rate conversion. Dropping a sample, or moving one back in the sample count represents a positive rate change. What we have described is sample rate conversion in order to align the transmitter and receiver data rates. As in the previous section, the timing error correction in the pulse shaped modem is asynchronous. Two methods can be considered: the adding and dropping of samples, as discussed in the previous section, and a new method [1,3] based on polyphase filter interpolation between the samples of the receiver response. In the first case, as described in the previous section, the timing error is allowed to build, until the timing phase mismatch is approximately one sample period long, and then a sample period is either added or dropped from the timing epoch following the decision. In systems with many samples per symbol, this is quite satisfactory. The adding or dropping of samples produces the required sample rate conversion to match transmitter and receiver data rate.

In systems with a more limited degree of oversampling, however, the timing offsets can grow to be quite significant fractions of a symbol period, and cause performance degradation [1]. Hence, a more precise way of controlling the timing error is desired. If a point on the response, in between the system sampling points were available, it would be desirable to move to this intermediate point instead. That kind of reasoning leads to timing correction by means of interpolation between sample points, which raises the effective sampling rate of the system, at least as far as the timing correction loop is concerned [1,3]. For a non-dispersive channel, a simple way to design such interpolators is given in [1]: simply design the receiver FIR matched, data filters to the desired oversampling rate, M, and then pick off M separate filters, by taking successive Mth taps out of the oversampled impulse response. In such a system the timing resolution is reduced to T_s/M where T_s is the received sampling period. In [1] this is termed filter coefficient interpolation.

Figures 3 and 4 represent DSP based results with and without filter coefficient interpolation based timing recovery. Note the increased timing resolution produced by filter coefficient interpolation. More details can be found in [4]. The case of a coherent BPSK voice rate modem was treated in [5].

III. EXPERIMENTS WITH RAISED COSINE PULSE SHAPED MODEMS

We will do our tests for the transmitter shown in Figure 5. Fading is introduced in the transmitter for our tests to be discussed later. For now we consider an AWGN channel.

In [2], Gardner introduces a non-decision aided (NDA) zero crossing tracker algorithm for Nyquist pulse shaped modems, which has the following form. The timing error measurement for the receiver in Figure 2 is given by

$$u(n) = x_I\left(n-\frac{1}{2}\right)[x_I(n)-x_I(n-1)] + x_Q\left(n-\frac{1}{2}\right)[x_Q(n)-x_Q(n-1)] \quad (1)$$

where $(x_I(n)\ ,\ x_Q(n))$ are the (inphase, quadrature) samples at symbol time n. This NDA variant of Gardner's

zero crossing tracker is shown in [4] to be free of self noise in the case of $\alpha = 100\%$ for any PSK data transition, and not just those with equal pulse heights [1]. Both variants of Gardner's zero crossing tracker can be adapted to operate with rectangular pulse shapes [4]. For $.6 \leq \alpha < 1$, intersymbol interference will occur on the mid-band samples in (1). This gives rise to timing jitter. The effect of this jitter is studied in [4] and it was found that excellent performance can be attained by smoothing $u(n)$ in (1) with a 50 Hz, first order, digital loop filter.

The MSAT signal standard will use Raised Cosine (RC) pulse shapes with $\alpha = 60\%$ and DQPSK modulation with conventional convolutional coding. As such, a family of 4800 bps modems has been developed with α ranging from 100% to 60%. Experimental performance testing has been carried out for the AWGN channel, that is for no fading in Figure 5. Figure 6 shows BER results for the 60% excess bandwidth case. Results for the 70%, 80%, 90% and 100% cases are similar [4] and are invariant with respect to excess bandwidth. In all cases, implementation losses are kept well under 1 dB. The timing synchronizer shows very good behaviour. Table 1 shows results for the worst case considered, with $\alpha = 0.6$, for three SNR's. It can be seen that at high SNR, there is an almost complete absence of jitter. More channel noise does induce some timing jitter, but even at an SNR corresponding to a BER on the order of 10^{-2}, the timing jitter is very low, with only 15 corrections in the wrong direction. We have also implemented the filter coefficient interpolation algorithm and similar performance was obtained.

IV. DOPPLER AND MOBILE FADING

The modems described so far have been developed for and tested experimentally on an additive white Gaussian noise channel which accurately describes only a stationary satellite link. On a mobile link, a clear line of sight to the satellite cannot be guaranteed, and some degree of multipath interference, or fading is inevitable. In addition, Doppler shifts of the carrier frequency occur as the vehicle on which the mobile unit is mounted accelerates, decelerates, or changes direction. A further complication arises when cheaper class C amplifiers are used with $\pi/4-$DQPSK modulation in order to save cost. Use of non-linear amplifiers leads to large amounts of spectral regrowth, and causes adjacent channel interference problems [7].

Doppler tracking techniques [5,6] have been incorporated into the RC pulse shaped modem described in the previous section. These techniques rely on rotating the received signal phasor to compensate for detected Doppler offsets. Since this rotation is carried out on the detected signal following the data filtering, it has no particular bearing on timing recovery, which has been demonstrated [4] to be immune to any phase offset if the NDA variant of the Gardner zero crossing tracker is used. Both closed- [5] and open-loop [6] algorithms have been studied. We have also included modification of the root-raised cosine pulse shaped transmitter portion of the modems to use $\pi/4-$DQPSK modulation which has been shown to minimize spectral regrowth [7].

The behaviour of the 4800 bps RC pulse shaped modem system on the multipath fading channel has been studied with the aid of computer simulations. The multipath fading model used in the simulations is Rician [8,9]. The fading was incorporated into the transmittor for testing as shown in Figure 5.

Simulation results on moderate fading channels with our original system configuration (DQPSK with open/closed Doppler tracking and ramp-varying Doppler factor corresponding to 40 Hz + /- 20Hz/sec.) are very poor: the timing recovery loop exhibits tremendous jitter, and does not provide any useful information, while the bit error rate is 50%. The cause of the jitter can be seen when the timing is frozen, and the mid-baud data filter outputs on the I and Q rails are plotted. As expected, it is found that there is severe distortion on the nominal zero crossing points when the fading is a constructive interference and gives a received signal well above the average level. On the other hand, a destructive deep fade, severely alleviates timing information. Hence the fading directly interferes with the operation of the zero crossing tracker timing error detector. Two separate modifications to the timing recovery loop have been implemented, both of which restore the functionality of the zero crossing detector making it useful on the fading channel. These modifications are based on deducing the presence of severe fading interference, either the constructive or destruction type, and the suppression of timing recovery while either type of fade is in progress. Since timing drift is a relatively slow phenomenon the receiver need not lose synchronization, unless the fade is of extremely long duration, which is so rare an event that it is impractical. Thus, we establish a window of signal ampli-

tude levels, centered about the mean signal level, in which timing error measurements will be computed from (1).

The first modification is to implement a zero-crossing threshold on the timing error signal in (1). If the nominal zero crossing point on either the I or Q rail is too large, timing corrections are not made. Timing is frozen until the zero crossing points are again within an acceptable range. After the thresholds are optimized, this modification yields the results shown in Figure 7, which are very close to those obtained with perfect timing, but are for timing jitter and a Doppler of 40 Hz. Figure 7 is for a Doppler shift of $B_d = 40$ Hz with a time variation of 20 Hz/sec. In both cases the time variation of the fading is due to a first-order Butterworth filter. The losses due to fading are larger for this filter than for higher order filters. For the Rayleigh ($K = 0$) case, the bound in equation (9.124) and Table 9.2 of [10] gives the BER floor as $4\pi B_d T$, for the first-order Butterworth filter and $.5(\pi B_d T)^2$ for the second order Butterworth case. Thus the first-order case has higher losses for the usual values of K.

The second modification involves continuously measuring the received signal power. An acceptable power level can be obtained by observing a fade-free signal. A severe fade either decreases the signal power as a result of destructive interference of multipath components, or increases it as a result of constructive interference. It is possible to implement an upper and lower signal envelope threshold defining an acceptable power range, and only perform timing measurement in (1) if the received signal power lies in that range. The average signal power depends on the $K-$factor, and the power thresholds have to be optimized over the expected range of operation, which in our case is for $K = 5$ dB to $K = 20$ dB. Again results very close to those given above for the timing error thresholding were obtained.

V. CONCLUSIONS

Fully digital, asynchronous timing recovery has been demonstrated to give excellent results in laboratory experiments on speech rate (2400 and 4800 bps) modems with RC pulse shaping. Gardner's zero crossing tracker timing error detector has been applied to RC pulse shaped speech rate modems with excellent results on the additive Gaussian noise and Rician fading channel. The NDA form of the zero crossing tracker has been found to be immune to pattern noise for any data phase transition, making it ideal for timing error detection in M-PSK and M-DPSK systems with $M > 4$. In RC pulse shaped systems with α down to 60% ISI induced self noise is sufficiently controlled by loop filtering. In addition, the NDA timing error detector is immune to phase offsets.

REFERENCES

[1] F.M. Gardner, "Demodulator Reference Recovery Techniques Suited for Digital Implementation", ESA Contract 6847/86/NL/DG, Final Report, May 16, 1988.

[2] F.M. Gardner, "A BPSK/QPSK Timing Error Detector for Sampled Receivers", *IEEE Trans. Comm.*, COM-34, pp.423–429, May 1986.

[3] M. Oerder and H. Meyer, "Digital Filter and Square Timing Recovery", *IEEE Trans. Comm.*, Vol. COM-36, pp. 605–611, May 1988.

[4] B. Koblents, "Asynchronous Timing Recovery in M-PSK Data Modems", M.Sc. Thesis, Queen's University, Kingston, Ontario, Canada, July 1988.

[5] P.J. McLane, W. Choy, T. Tay, "Filter Coefficient Interpolated Timing Recovery in Sampled Coherent PSK Receivers", *Globecom '92.*

[6] M.K. Simon and D. Divsalar, "Doppler-Corrected Differential Detection of MPSK", *IEEE Transactions on Communications*, Vol. 37, pp. 99–110, February 1989.

[7] S.N. Crozier, "A Comparison of Three QPSK Type Modulation Schemes for Mobile Satellite SCPC Voice and Data Services", *16th Biennial Symposium on Communications*, Kingston, Ontario, Canada, May 27–29, 1992.

[8] K.A. Norton, L.E. Voler, W.V. Mansfield, and P.J. Short, " The Probability Distribution of the Amplitude of a Constant Vector Plus a Rayleigh Distributed Vector", *Proceedings of the IRE*, Vol. 43, pp. 1354–1361, Oct. 1955.

[9] G.T. Irvine and P.J. McLane, "Symbol-Aided Plus Decision-Directed Reception for PSK/TCM Modulation on Shadowed Mobile Satellite Fading Channels", *IEEE Journal on Selected Areas in Communication*, Vol. 10, No. 8, pp. 1289–1299, October 1992.

[10] E. Biglieri, D. Divsalar, P.J. McLane and M. K. Simon, "Introduction to Trellis-Coded Modulation with Applications", Macmillan 1991.

2,097,152 SYMBOLS			
SNR, $2E_b/N_o$, dB	14.9	12.5	9.5
BER	1.2×10^{-5}	1.2×10^{-4}	1.2×10^{-2}
Forward Corrections	30	42	59
Backward Corrections	0	1	15
Net Number of Corrections	30	41	44

Table 1: Numbers of timing corrections at high, moderate and low SNR.

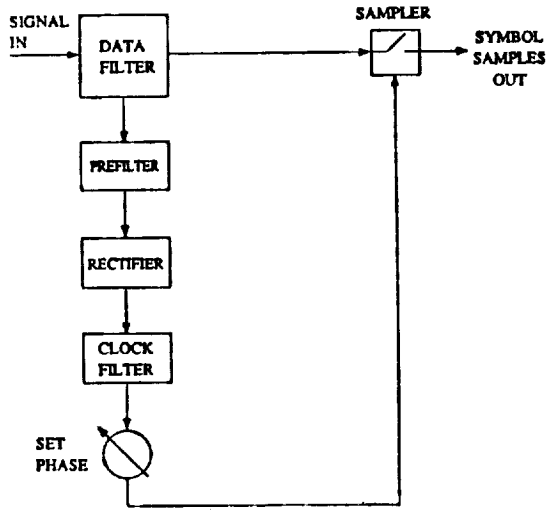

Figure 1: Feedforward clock recovery.

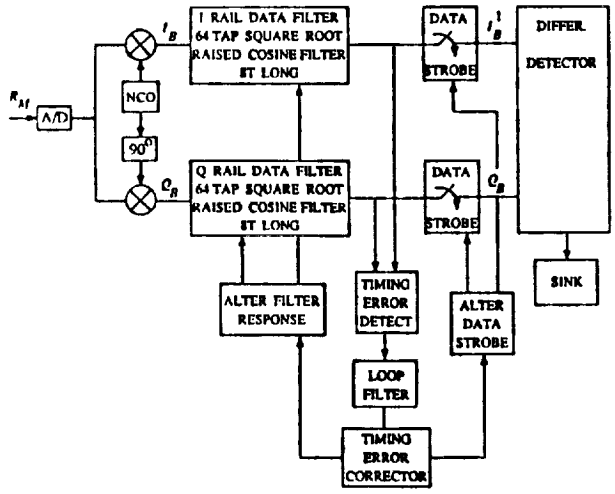

Figure 2: 4800 bps raised cosine pulse shaped modem receiver block diagram.

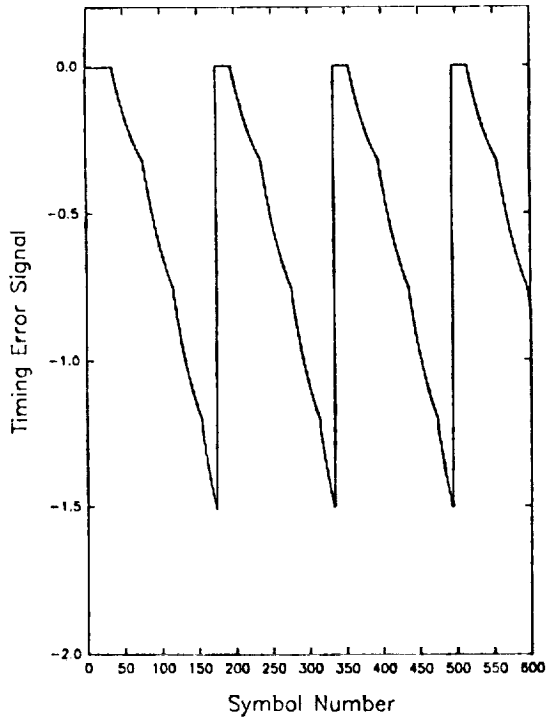

Figure 3: Timing error signal for simulated pulse shaped modem with timing correction by adding and dropping samples only. Timing drift: same as for Figure 4.

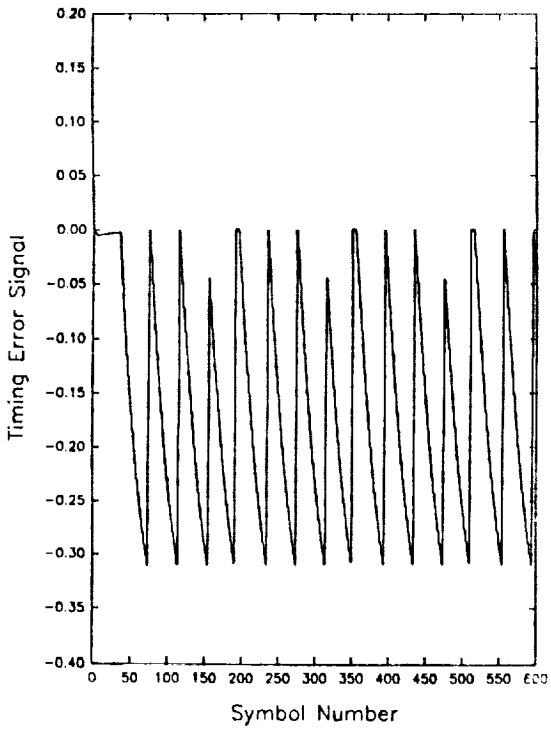

Figure 4: Timing error signal for simulated pulse shaped modem with coefficient interpolation timing recovery. Timing drift: transmitter filters permuted every 30 symbols, sample dropped every 120 symbols.

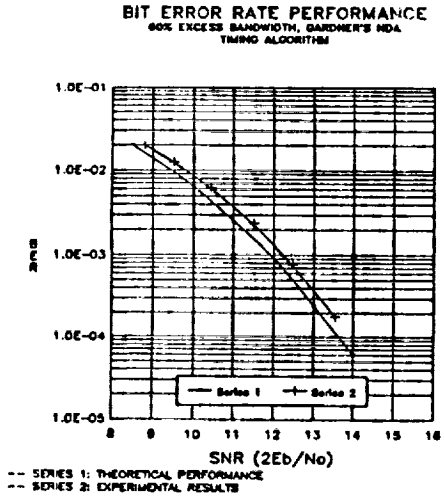

Figure 6: BER performance for 60% excess bandwidth, 4800 bps raised cosine pulse shaped DQPSK modem.

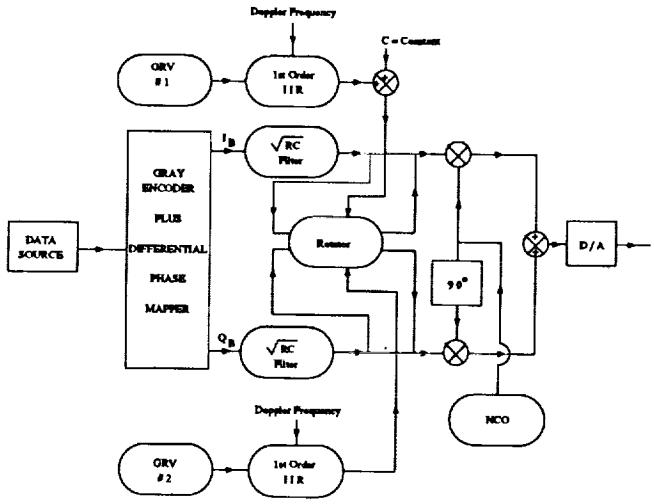

Figure 5: Block diagram of transmitter that includes fading for system testing.

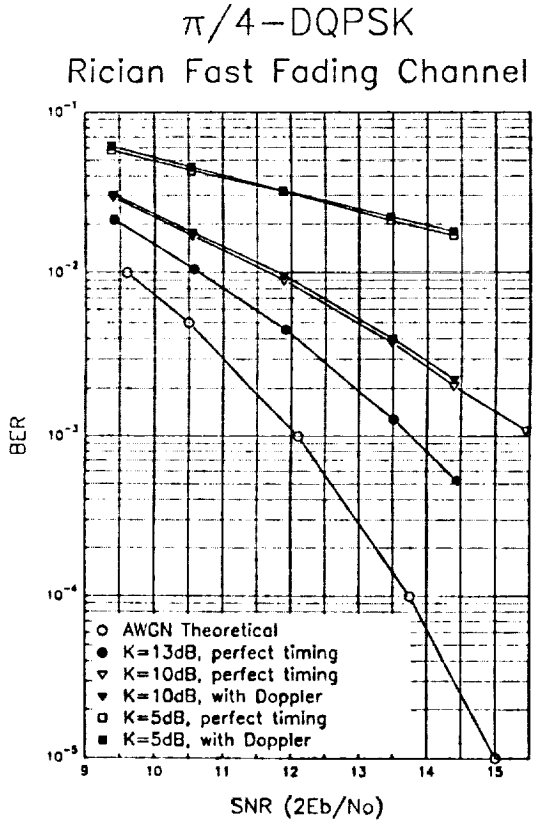

Figure 7: BER performance for a 40 Hz Rician Fast Fading channel with a first order Butterworth Doppler filter and with a time-varying 40 Hz Doppler offset.